Journal of Hazardous Materials 480 (2024) 135982

Contents lists available at ScienceDirect

Journal of Hazardous Materials

journal homepage: www.elsevier.com/locate/jhazmat

Research Article

Investigating the deposition of fibrous zeolite particles on leaf surfaces: A novel low-cost method for detecting the presence of airborne hazardous mineral fibers

Wenxia (Wendy) Fan [a,*], Alessandro F. Gualtieri [b], Kim N. Dirks [c], Paul G. Young [d], Jennifer A. Salmond [a]

[a] School of Environment, Faculty of Science, University of Auckland, Auckland, New Zealand
[b] Department of Chemical and Geological Sciences, University of Modena and Reggio Emilia, Via G. Campi 103, 41125, Modena, Italy
[c] Department of Civil and Environment Engineering, Faculty of Engineering, University of Auckland, Auckland, New Zealand
[d] School of Biological Sciences, Faculty of Science, University of Auckland, Auckland, New Zealand

HIGHLIGHTS

- Quantifying the dispersion of airborne fibers from hazardous minerals (including some zeolites) is challenging.
- A novel cost-effective method for identifying the airborne dispersion of zeolite fibers onto leaves is presented.
- Morphological analysis showed that zeolite particles could be detected and characterized on leaves from 80 % of sampling sites.
- The presence of mordenite was confirmed using elemental composition and novel crystallographic techniques.

GRAPHICAL ABSTRACT

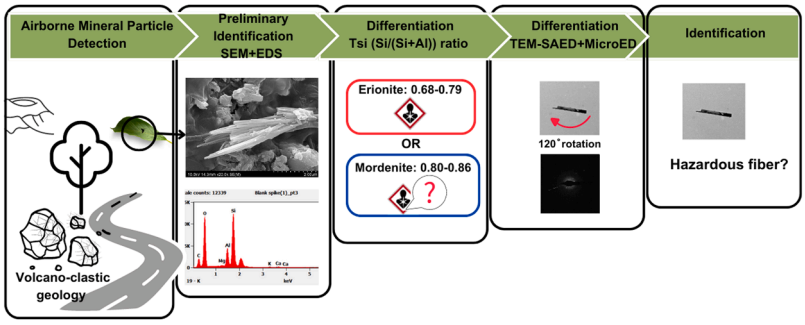

ARTICLE INFO

Keywords:
Naturally occurring fibrous zeolites
Erionite
Mordenite
Leaf surface sampling
Continuous rotating electron diffraction

ABSTRACT

Naturally occurring fibrous minerals, such as erionite, can pose a significant threat to human health when disturbed and subsequently respired. Understanding the spatial abundance and characteristics of these hazardous fibrous minerals in ambient air is crucial for minimizing human exposure and assessing risk. Conventional detection methods for airborne hazardous mineral fibers, such as those developed for asbestos, are of limited utility in environmental settings where fiber concentrations are low and different fiber types may be present and can be costly especially when monitoring large areas over long periods of time. This study presents an innovative methodology for detecting and identifying the presence of airborne naturally occurring fibrous zeolites, using

List of Abbreviations: ISO, International Standard Organization; NIOSH, National Institute for Occupational Safety and Health; XRPD, X-ray powder diffraction; EPMA, Electron probe microanalysis; TEM, Transmission electron microscopy; SAED, Select area electron diffraction; PCM, Phase contrast microscopy; 2D, Two-dimensional; SEM, Scanning electron microscope; EDS, Energy-dispersive spectrometer; SEM-EDX, Scanning electron microscopy energy-dispersive X-ray spectrometry; TEM-SAED, Transmission electron microscope selected area electron diffraction; Si, Silica; Al, Aluminum; Na, Sodium; K, Potassium; Ca, Calcium; ED, Electron diffraction; MicroED, Microcrystal electron diffraction; SMV, Super Marty View; XDS, X-ray detector software; FZPs, Fibrous zeolite particles; Mg, Magnesium.

* Corresponding author.
E-mail address: wendy.fan@auckland.ac.nz (W.(W. Fan).

https://doi.org/10.1016/j.jhazmat.2024.135982
Received 24 April 2024; Received in revised form 22 September 2024; Accepted 25 September 2024
Available online 26 September 2024

leaf surface deposition sampling, SEM-EDX analysis for the detection and assessment of elemental composition, and TEM-SAED with continuous rotation diffraction (MicroED) to determine their crystallographic unit cell parameters. In total, 309 fibrous zeolite particles (FZPs) were identified on a range of tree leaf surfaces across 80 % of the sampling sites located close to both active and disused zeolite quarries in the Taupo Volcanic Region, New Zealand. The FZPs displayed various morphologies including aggregates, bundles, and fibril-like structures. Of the FZPs detected, 92.2 % were < 5 μm in length. Tetrahedral Si:(Si+Al) ratio results indicated that 40 % of the FZPs were in the reference range for zeolite mordenite. TEM-SAED plus MicroED analysis resulted in 61 % of tested FZPs indexed to unit cell parameters that matched with mordenite. This research demonstrates the potential of leaf sampling as a cost-effective method for detecting airborne FZPs while the MicroED data can be utilized for distinguishing between different types of airborne fibrous zeolites in ambient air.

1. Introduction

Naturally occurring zeolites are comprised of more than 50 aluminosilicates that are commonly found in regions with volcano-clastic geology, and some of which have a wide range of industrial applications [1–3]. While most naturally occurring zeolites are found in crystalline habits with platy, equant, or fibrous morphologies, a small number of them exhibit the finely fibrous-asbestiform shape that could pose health hazards if inhaled [4,5]. These include fibrous forms of erionite, mordenite, offretite, and ferrietite [6–10]. Fibrous erionite and mordenite are among the top five most abundant naturally occurring zeolites (namely clinoptilolite, phillipsite, chabazite, mordenite and erionite) and are commonly found in sedimentary deposits near the earth's surface[4]. When disturbed by natural processes (e.g., weathering, earth quakes and landslides) or anthropogenic activities (e.g., mining, excavation works for roads or buildings and recreational activities such as mountain biking), fibers may become airborne, posing a risk to human health, especially if they display respirable size [4,11,12].

To date, amongst fibrous zeolites, only erionite has been classified as a *Group 1* carcinogen, as epidemiological data has linked erionite exposure to a malignant mesothelioma epidemic in Cappadocia, Turkey, during the 1970s [13–15]. Furthermore, experimental data have indicated that fibrous erionite exhibits higher tumorigenic potential in rodents compared to crocidolite and chrysotile [16,17]. Despite sharing a high level of similarity in chemical-physical properties, the hazardousness and carcinogenic potential of fibrous zeolites other than erionite remain uncertain and require further investigation [6,9,10,18]. As a matter of fact, none of the fibrous zeolites (including erionite) are regulated to date.

Given the potential health risks of exposure to these common fibrous zeolites, careful ambient monitoring for their prevalence is essential for assessing and mitigating the potential health risks, especially in populated areas where such fibers are prevalent near the earth's surface. However, despite the importance of understanding the controls on the suspension and the dispersion of zeolite fibers in ambient air, there are very few studies available (and all limited to erionite) to draw upon, and no standard methodological approaches for measuring the ambient concentrations of zeolite fibers have been established.

Instead, previous studies have drawn on the regulatory methodologies for measuring airborne asbestos (chrysotile, asbestos actinolite, amosite, asbestos anthophyllite, crocidolite and asbestos tremolite) fibers as a starting point for the development for measurement methods for erionite [7,19]. Typically, study methodologies involve pumping airborne particles onto a filter using a standardized flow rate and sampling volume as outlined in the NIOSH 7400; 7402, International Standard Organization 10312; 13794 [20–22]. However, this detection method, whilst shown to be effective in confined areas and for measuring personal exposure during activities for erionite, it is less effective in outdoor environments where concentrations are low or temporally or spatially variable, despite the abundance of erionite-containing rock and soil sources near the ground surface [7,19,23].

Assuming that zeolite fibers can be successfully captured and isolated from a filter sampling system, further methodological challenges remain. Research on regulated asbestos fibers has shown a positive correlation between fiber length and toxicity [24,25]. Consequently, the hazardous respirable fiber criteria, for example, as set in the World Health Organization guidelines, as length greater than 5 μm; width smaller than 3 μm, and an aspect ratio (length/width) greater than three [12]. Fibers which meet these specifications are typically counted in asbestos exposure monitoring studies.

However, unlike asbestos, erionite fibers are fragile and easily broken. Previous studies carried out in Turkey and in the US have reported the size distribution of airborne erionite as consisting of thinner and shorter fibers with aspect ratios greater than three; a length range from 0.56 to 38 μm (with a mean of 3.57 μm) and a width range from 0.06 to 5.04 μm (with a mean 0.31 μm) [7,19,26]. However, depending on their geological formation, natural fibrous zeolites occur in various habits, resulting in diverse morphologies and size distribution across different regions [6,27–29]. Furthermore, airborne fibers may be subject to weathering, erosion and breakage, especially in light of their fragility. Thus, the size criteria alone may not be a good indicator for detecting the presence of airborne erionite specifically or zeolite fibers generally.

In addition to detecting the size and shape of respirable fibers on filter paper, given the range and unquantified toxicity of different zeolites present in environmental settings, it is important to ascertain what type of zeolite fiber has been captured. To add to the complexity, natural zeolite fibers rarely occur in pure form, commonly co-existing with other zeolite minerals [29–31]. Identifying erionite from mordenite and offretite is especially challenging, and problematic for regions such as New Zealand where they have been found occur together [30]. Techniques such as X-ray Powder Diffraction (XRPD) and Electron Probe Microanalysis (EPMA), commonly used to determine the crystallographic data and chemical composition of zeolites in geological applications, are of limited use in air samples where the sample sizes are comparatively tiny [27,32,33].

As a result, previous studies which sought to quantify ambient concentrations of erionite (e.g., studies carried out in Turkey and in the USA) only utilized elemental composition data (energy dispersive X-ray spectrometry (EDX)) and morphology (elongate shape, aspect ratio greater than three) to identify fibrous erionite, justified by the confirmed abundance of erionite-containing sources found in the studies areas [7,19,26]. However, such a methodology may not effectively isolate erionite fibers from other zeolites present such as mordenite. The elemental composition data is essential for differentiating zeolite fibers from other mineral fibers in the environment, but it cannot be conclusive for erionite identification, given its good ion exchange capacity, excellent adsorption ability, and its high level of similarity in elemental composition to other fibrous zeolites such as mordenite and offretite [34,35].

To identify the type of zeolite present, utilizing differences in crystallographic spacing parameters has been suggested as a reliable method for differentiating individual fibrous erionite from other fibrous zeolites [27,34,35]. However, zeolites in general are highly sensitive to electron beams, and it has been observed that they can rapidly transform from crystalline to amorphous form, making it challenging to manually tilt the sample and obtain a highly symmetric electron diffraction pattern for identification [36–38]. Furthermore, interpreting electron

diffraction patterns requires specialized mineralogical indexing knowledge and no study yet so far goes to this extent to analyze airborne zeolite fibers detected [19,26,27].

As a result of the difficulties and expense of existing airborne fiber sampling methodologies, little is known about the suspension rates, residence time or likely dispersion patterns of zeolite fibers. There are essentially no data related to the dispersion of aerosolized zeolite fibers in regions with a non-arid climate or abundant vegetation, such as New Zealand. To date, it is unclear whether respirable sized fibers are released and dispersed in ambient air by environmental processes in areas with naturally occurring geological deposits [31,39,40].

This paper focuses on developing a low-cost method for detecting the likely presence of naturally occurring airborne hazardous mineral fibers in ambient air. While we understand the importance of quantifying airborne fiber concentrations and hence exposure levels, our goal here was to establish a low-cost and reliable technique for detecting the presence / absence of these fibers which often occur in low concentrations in the outdoor environment. This preliminary activity serves as the first step in identifying areas for subsequent quantitative risk assessments.

This novel airborne hazardous mineral fiber screening method draws on the wealth of existing literature relating to the deposition of ambient particulate matter on vegetation [41–43]. Previous studies have shown that tree leaves can effectively capture ambient particulate matters with diameters of less than 10 μm and retain them on their surfaces in various capacities based on their surface features [44–46]. Thin fibers possessing larger surface areas compared to round-shaped particles, may adhere more firmly to leaf surfaces once settled, making them less prone to being shaken off compared to larger, round sand or clay particles [47, 48].

It was therefore hypothesized that if zeolite fibers were present in the atmosphere, they should be detectable on leaf surfaces in the vicinity of the source. The advantage of this technique is that areas can be screened for the possible presence of airborne zeolite fibers without the requirement for expensive, labor intensive ambient sampling campaigns, and if a positive result is found on a leaf surface, more expensive quantitative filter-based sampling can be targeted at the appropriate sites.

Two analytical techniques, scanning electron microscopy with energy dispersive X-ray spectroscopy (SEM-EDX) and transmission electron microscopy with selected area electron diffraction (TEM-SAED) were employed to differentiate the types of zeolite fibers found in this study. To address the uncertainties in elemental composition, the tetrahedral Si:(Si+Al) ratio (Tsi or R ratio) was used for differentiating fibrous zeolites based on the stability of Si and Al detection levels in EDX analysis [49,50]. To further confirm zeolite type, a novel form of TEM-SAED coupled with Micro Electron diffraction (MicroED) was used to determine the cell parameters of the zeolite fibers. MicroED is a technique that enables fast, high resolution structural determination and is predominately used for determining the crystallographic structures of small molecules and proteins [51–53]. Diffraction data are continuously collected in movie mode, and the electron diffraction data indexed with Xray diffraction software (XDS) to generate crystallographic spacing parameters [35,40,52,50]. The methods were calibrated using bulk samples that had previously been confirmed as containing either erionite or mordenite for comparison.

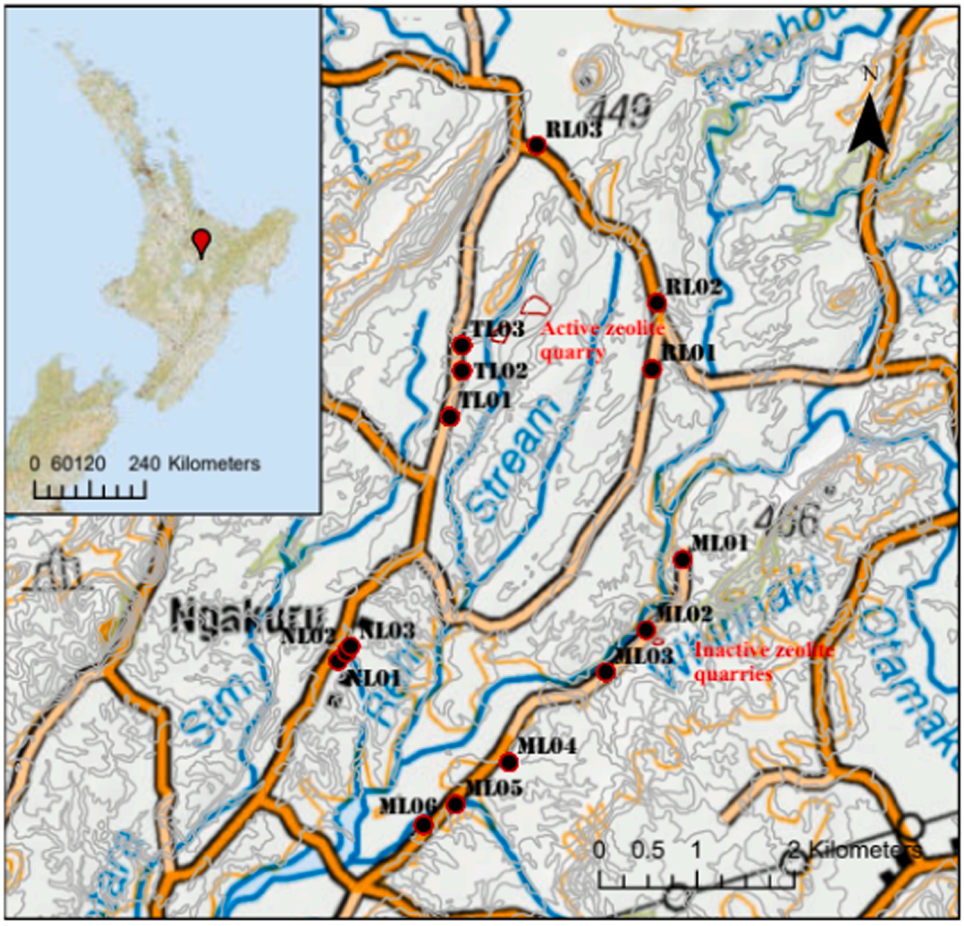

Fig. 1. Map of 15 sampling stations, ML01-ML06 on the Mangatete Road; NL01– NL03 in the Ngakuru Town area; TL01–TL03 on the Twist Road; RL01–RL03 on the Rehi Road. Grey lines indicate the contour lines of the area (NZ Contours (Topo, 1: 50 k), Land Information New Zealand)[57].

2. Materials and methods

2.1. Sampling locations

The sampling stations were situated in the Ngakuru area within the Taupo Volcanic Zone, in the Waikato Region of the North Island, New Zealand (Fig. 1). In this area, zeolite deposits, including those of mordenite and clinoptilolite were mined in three zeolite quarries (Fig. 1). Among these quarries, one remains actively operational as an open-cast quarry on Twist Road, producing an annual output of 50,000 to 60,000 tons of zeolite (Clinoptilolite and mordenite) [54]. The other two quarries, located on Mangatete Road, are currently inactive, and comparatively smaller in scale [55]. Notably, erionite occurrence has also been reported in the Ngakuru area [56].

The Ngakuru area has a mild temperate climate. The land in the area is used mainly for dairy farms and commercial forestry, with most of the soil covered by vegetation. The Twist Road quarry (active) is surrounded by large tree acting as barriers. The Mangatete Road quarries (non-active) have visible outcrops of zeolitic rocks.

2.2. Leaf samples collection

To detect the presence of air dispersed fibrous zeolites, sampling was conducted following periods of rain to minimize potential overloading of leaf surfaces by aerosolized coarse dust or soil particles. Sampling commenced on March 15, 2023, during sunny weather with a temperature of 23.5 °C, and a wind speed of 2.5 m/s. The soil moisture (at the depth of 20 cm) was 32.6 %, indicating near saturation and reducing the likelihood of soil particle aerosolization (National Institute of Water and Atmospheric (NIWA)) [58]. Recent rainfall events included a heavy rainfall event (26.6 mm) on March 5, 2023, and light drizzle (1.4 mm) on March 13, 2023, prior to sampling [58].

A total of 15 sampling locations were selected, as shown in Fig. 1. Six were located along Twist Road (TL01 to 03) and Rehi Road (RL 01 to 03), near the active Twist Road zeolite quarry, while a further six were located along Mangatete Road (ML01 to ML06), near the non-active Mangatete Road quarries [55]. Finally, three of the sampling locations were located in the Ngakuru Town center area (NL01 to NL 03). All sampling stations were located alongside sealed roads.

At each location, woody plant foliage (consisting of varied species depending on the local availability) facing toward the road were collected at heights of 1 – 1.2 m from the ground, corresponding to the general breathing-zone height, as well as typical of the breathing height for drivers in cars. Three replicates of leaf samples were collected at each location, each placed in separate labelled petri dishes. These samples were then put into air-tight plastic containers and carefully transferred and stored in a laboratory freezer (−18 °C) to prevent decomposition. The storage of samples in a freezer over a period of a month or more initiates a slow dehydration process, preserving the leaves' flat surface shape, make them suitable for subsequent electron microscope analysis.

2.3. Erionite and mordenite containing bulk samples

For comparison purposes, erionite-containing bulk samples (confirmed by XRPD analysis, as reported in S1 in the Supporting Information) from the Timber Bay formation, Kaipara, North Island, New Zealand [30,59], as well as mordenite-containing bulk samples (confirmed by XRPD analysis, as reported in S2 in the Supporting Information) from Ngakuru, Taupo Volcanic Zone, New Zealand [55] have been analyzed in the same manner as the unknown fibrous zeolites particles from leaf surfaces.

2.4. Detection and preliminary identification of fibrous zeolites

To detect and identify fibrous zeolite on leaf samples, SEM coupled with EDX analysis was conducted, a common methodology for analyzing mineral fibers and micro- and nanoparticles [35,49,60,61]. The leaf samples, dehydrated for at least a month in the freezer, were taken out and cut into suitable sizes (with the areas ranging from 2.62 to 128 mm^2), and mounted on SEM stubs (with the adaxial side up), using double-sided conductive carbon tape under a fume hood. Initial trials revealed no mineral particles detection on the leaf samples mounted with the abaxial side up. The samples on the SEM stubs were then further dried at room temperature for three days inside a plastic box under a fume hood. Subsequently, each leaf sample was sputter-coated for 100 s with platinum (Pt) using a Hitachi E-1045 (Hitachi Ltd).

A Hitachi SU-70 Schottky field emission scanning electron microscopy (SEM), coupled with a dispersive X-ray spectrometer (EDS) with a Noran System 7 (NSS) microanalysis system, was then used for detection and elemental composition analysis. The EDS accelerating voltage was set to 15 kV, and the acquisition time was 60 s

The detection criteria in this study for fibrous zeolites involved both morphological characteristics and elemental composition. Morphologically, the particles exhibited a fine, consistently elongated shape (with the aspect ratio being $>$ 3:1); or particles (in the shape of bundle or aggregate) that contain these fine, consistently elongated shaped fibrils. Furthermore, their EDX spectra display main peaks of silicon (Si) and aluminum (Al), along with minor peaks containing one of sodium (Na), potassium (K) and calcium (Ca) [26,35].

Fibrous particles were first identified as zeolites, and then compared with bulk samples of erionite and mordenite, depending on the particle size, with either single or multiple points selected for collecting elemental composition data via EDX. However, due to the potential environmental contamination of airborne samples, and their small sizes, and the potential impact of signals from leaf surfaces that may also be detected by EDX, the spectra produced are often not as clear or easily comparable as the spectra from bulk samples. Given the similarity in elemental composition between some zeolites, especially carcinogenic erionite and the less harmful mordenite, the EDX spectrum alone cannot be used to conclusively differentiate between the three fibrous zeolites for these samples [35].

To distinguish erionite from other fibrous zeolite using SEM-EDX, the tetrahedral (Tsi) ratio (Si/(Si+Al)) was used as an indicator in this study [6,19,62,63]. It has been suggested in previous mineralogical studies that compared to other elements (K, Na, and Ca), Si and Al demonstrate relatively stable signals in smaller zeolite particles (diameter $<$ 10 μm) compared to bulk samples in results from EDX [49]. The elemental weight percentages (wt%) for the Tsi ratio calculation were obtained from the most reliable point, typically chosen on a relatively flat surface and in the geometrical center of the particle. The EDX spectra and Tsi ratios of fibrous particles from leaf surfaces were compared with literature data (Table 1) and with bulk samples containing mordenite and erionite analyzed in the same SEM-EDX settings.

2.5. Measurement of fibrous zeolite particles size

In this study, FZPs detected under SEM, following both morphological and elemental composition detection criteria, were captured in micrographs. These images were processed and measured in ImageJ software (*Version 1.53g62*) [64]. Since fibrous zeolites are naturally occurring and may appear as irregularly shaped particles, measuring the morphometric parameters of these particles is challenging. The maximum and minimum caliper lengths were used in a previous study for volcanic clast particles in SEM image analysis [65]. To facilitate

Table 1
Elemental composition and Tsi ratio of three fibrous zeolites [50].

Zeolite	Ideal chemical formula	Tsi Si/(Si+Al) ratio
erionite	$K_2(Na,Ca_{0.5})_8[Al_{10}Si_{26}O_{72}]\bullet 30H_2O$	0.68 – 0.79
mordenite	$(Na_2,Ca,K_2)_4[Al_8Si_{40}O_{96}]\bullet 28H_2O$	0.80 – 0.86
offretite	$CaKMg[Al_5Si_{13}O_{36}]\bullet 16H_2O$	0.69 – 0.74

efficient measurements, we utilized ImageJ's built-in measurement settings, and used the maximum and minimum ferret's diameter as the length and width to reflect the size of the FZPs. These dimension measurements are similar to the caliper lengths noted in Bagheri *et al.* (2015) [65]. The aspect ratio of each FZP was calculated by dividing its length by its width.

2.6. Relative abundance of fibrous zeolites on leaf surfaces

Searching and counting all microscale and sub-microscale particles on the whole of a leaf surface sample (area ranging from 75 to 2020 mm^2) through SEM analysis is time-consuming. To efficiently estimate the abundance of fibrous zeolites and facilitate comparison across different sampling locations, a quadrant sampling technique was used, common in ecological studies for estimating the population density of plant and animals in a region [66,67]. In this study, for leaf samples from each sampling location, six random 0.1 mm^2 plots were selected for analysis. The images of these plots were captured using 400x magnification of SEM. We conducted searching the FZPs using higher magnification, and captured the micrographs of the FZP in each plot. These micrographs were processed in ImageJ software to count the number of fibrous particles in each 0.1 μm^2 plot. The FZP level for each sampling location was calculated using the following equation:

$$L_f = \frac{\sum n_p}{N_p} \times 100 \quad (1)$$

where L_f indicates the number of FZPs on the leaf surface at each sampling location (n/cm^2), consistent with the unit used for asbestos surface sampling; n_p denotes the FZP number count in each plot (of 0.1 mm^2) while N_p denotes the total number of analyzed plots. Because these fibers were observed in their original air-dispersed state, some individual particles may have overlapped as agglomerates. In this case, it was counted as one "aggregate" particle, referencing the counting rule for asbestos from the National Institute for Occupational Safety and Health (NIOSH) 7400 [20].

2.7. Identification of fibrous zeolites using crystallographic data

Erionite occurrence has previously been reported in the Ngakuru area [56]. To further confirm the type of zeolite found, and cross-validate the SEM-EDX identification based elemental composition data, a more reliable identification technique is crucial for accurate analysis [34,35,56]. Electron diffraction (ED) is a technique commonly employed to identify the crystallographic parameters of crystalline phases. Erionite, in particular, exhibits distinctive *c*-axis spacing of 15 Å, which differs from that of other fibrous zeolites (e.g., offretite and mordenite) (Table 2). This parameter has been proposed as a key indicator for identifying erionite [35]. Hence, TEM coupled with SAED analysis was employed in this study to collect the crystallographic data of FZPs detected on leaf surface. A field emission TEM (200 kV), Tecnai F20 (FEI Company) was used to collect ED data in this study.

Crystallographic data were collected using two methodologies. The direct transfer method involved transferring FZPs from the leaf surface directly to a TEM grid, with ED data collected under cryogenic conditions [33,35]. This approach is suitable for samples with high FZP abundance, reducing chemical contamination and electron damage while maintaining fiber stability for subsequent EDS analysis.

Table 2
Crystal cell spacing parameters of three fibrous zeolites (62,68).

Zeolite	*a* (Å)	*b* (Å)	*c* (Å)	*α* (°)	*β* (°)	*γ* (°)
erionite	≈ 13.3	≈ 13.3	≈ 15.1	90	90	120
mordenite	≈ 18.1	≈ 20.3	≈ 7.5	90	90	90
offretite	≈ 13.3	≈ 13.3	≈ 7.6	90	90	120

The indirect transfer method involved washing and concentrating FZPs from the leaf surface, followed by an organic removal process and then transfer to a TEM grid, with ED data collected at room temperature and a higher electron dose. This method is effective for samples with low FZP abundance, providing time-efficient characterization and higher-resolution diffraction for better fiber indexing and identification.

2.7.1. Direct transfer method

To prepare the samples for TEM analysis, the particles deposited on the sample leaf surfaces were transferred to a carbon film supported TEM copper grid (400 mesh). This was done by using a pre-washed clean, stainless steel micro lab spatula (with a flat square end), which was pre-wetted in ethanol (ECP-Analytical Reagent). The surface of the leaf sample was gently scratched with the spatula, and then the spatula was rinsed in 1 mL of ethanol in a 2 mL plastic test tube. Subsequently, the ethanol liquid containing the particles was dropped onto the TEM grid using a mechanical 0.1 to 2.5 μL pipette. This process was repeated five times for each grid, to ensure sufficient FZPs on the grid. The bulk samples that contained mordenite and erionite were prepared separately. The bulk samples were in powder form, and a pre-cleaned lab spatula was used to transfer a small amount of rock powder into 1 mL of ethanol in a 2 mL plastic test tube. The liquid containing the bulk samples in the tube was placed in a sonicator for 2 min and then dropped onto TEM grids using a pipette following the same procedure as for the leaf surface samples [69].

Some zeolites, including erionite and mordenite, are known to be highly sensitive to electron beam radiation, they have been observed to turn very quickly from crystalline form (producing diffraction data) to amorphous (no diffraction produced) [19,35,36]. To mitigate potential radiation damage, electron diffraction data was collected using cryo-MicroED and a TEM low-dose mode. MicroED is more commonly used for determining the crystallographic structure of very small and thin 3D crystals of small molecules and proteins and has had limited use in examining environmental mineral samples [51–53].

The sample was mounted in a high tilt cryo-holder and cooled with liquid nitrogen to ~ 100 K [19,34,35]. Samples were examined in low-dose search mode (1700 X magnification) to isolate fine and consistently elongated single particles (AR > 3:1, width < 0.3 μm). Electron diffraction data were collected from fibers in low-dose exposure mode (spot size 10) with a 200 μm select area aperture inserted and a virtual camera distance of 975 mm, which gives a potential resolution of 0.75 Å. Data were collected on a TVIPS 16k CMOS camera using a rolling shutter mode to collect 200 continuous exposures while the grid was rotated through 120 degrees (−60° to 60°). A TVIPS detector control module (MicroED.exe) was used to control the speed of the cryo-holder rotation so that each of the exposure frames (1.6 s) equated to 0.6 degrees of fiber rotation [70].

2.7.2. Indirect transfer method

To prepare the leaf samples for the indirect transfer method, a sample extraction and organic removal process was performed, which is a technique that has been modified from atmospheric microplastic studies to effectively remove organic material while minimizing damage to the remaining particles [71,72]. Whole leaf samples were washed using 100 mL of Type 1 water (Sartorius, 18.2 MΩ cm) in 200 mL beakers and sonicated for 5 min. The aliquots were then filtered onto a polycarbonate track-etched (PCTE) membrane filter (0.2 μm pore size, 47 mm diameter, Sterlitech), followed by rinsing the leaf three times with 200 mL of Type 1 water and filtering onto the same filter.

The PC membrane was then placed back in the beaker, and 30 mL of 30 % hyrogen peroxide (analytical reagent grade, Fisher Scientific) was added. The beakers were kept at room temperature in a fume hood for 48 h, followed by heating at 90 °C for 8 h. Subsequently, 100 mL of Type 1 water was added, and the aliquots in the beaker were sonicated for 5 min before being filtered onto new PCTE membranes filters, which were then dried in petri dishes under a fume hood for a week. A control

was conducted throughout the digestion and filtration process and analyzed under SEM to ensure any potential contamination or introduction of fibers from the laboratory environment was detected.

To prepare a TEM grid, a quarter of the sample filter was cut using a sterile scalpel and placed in a 2 mL plastic test tube. Next, 1.5 mL of ethanol (absolute for analysis, Supelco) was added to the tube, and the sample was sonicated for 2 min. The sample filter was then removed from the test tube. In the indirect transfer method, 300 mesh porous carbon film copper TEM grids (1.2 μm hole diameter, Protochips) were used to prevent ethanol coating on the FZP surface. The drop-casting TEM grid preparation followed the same process as the direct transfer method. The erionite-containing bulk samples were resuspended in ethanol and added to TEM grids as described above.

The sample grid was mounted in the same sample holder, and data were collected as described above for the direct transfer cryo-methodology, with the following changes. Data were collected at room temperature using a higher electron dose (spot size 7 instead of spot size 10) and with a smaller 40 μm sample aperture inserted. The grid was rotated 100 degrees (−40 to 60) with 170 continuous exposure. This adjustment increased the electron beam intensity, and the reduced aperture size improved the signal-to-noise ratio of the collected diffraction data.

2.7.3. Data analysis

Electron diffraction data collected in Tagged Image Format (.tiff) were converted into Super Marty View (SMV) X-ray image format (.img) using the program EM2EM (http://www.ImageScience.de/em2em) for subsequent processing with Xray crystallographic software. All images were manually inspected using (ADXV) (http://www.scripps.edu/tainer/arvai/adxv.html) and the beam center was recorded for each dataset. X-ray Detector Software developed for the integration of macromolecular Xray diffraction data (XDS) [52] was used to index and assign a potential space group and unit-cell parameters in angstrom and degrees (a, b, c and α, β, γ), and integrate the data (examples of indexing results can be found in S3 to S6 in the Supporting Information) [52,73]. During indexing, XDS lists a range of potential unit cell constant solutions with an associated quality of fit. While space group identification is attempted by XDS, the quality of fit measurement may not be reliable for ED data due to the presence of multiple scattering effects (dynamical effects). To account for this, the data were re-indexed and integrated in any crystallographic unit cell constants listed that matched known fibrous zeolites, and integration statistics were used to determine the most likely solution. These statistics are listed in the Correct.lp output. In general, integrated data can be expected to have an average signal to noise ratio (I/sigma) of > 2 with an overall R-measure (indicator of data consistency- agreement of symmetry related reflections) below 0.8. Only data in resolution shells with a cross correlation (CC 1/2) of greater than 50 % should be included. The data should be truncated to remove weak, unreliable high-resolution data to maximize data quality and confidence in indexing.

3. Results and discussion

A total of 309 fibrous zeolite particles (FZPs) that met the identification criteria were detected on the tree leaf samples from 12 out of the 15 roadside sampling stations in this study. The Tsi ratio calculated using SEM-EDX results allowed for the preliminary differentiation of zeolites. Moreover, the TEM-SAED technique, MicroED, enabled the assignment of the crystallographic cell parameters for single fibers, enhancing the accuracy of the identification of individual fibrous zeolite minerals, such as erionite and mordenite. This integrated methodology provides a clearer picture of the characteristics of airborne FZPs in the roadside environments in Ngakuru, New Zealand.

3.1. Morphology

Diverse morphologies were observed among the FZPs identified in this study, ranging from partially fibrous aggregates to fiber bundles and individual fibril-like structures. As shown in Fig. 2, the fibrous zeolite aggregates (Images A and B) accounted for 14 % of the FZPs observed. These fibrous aggregates contain multiple fiber bundles with numerous fibrils, some also incorporating solid, rocky components. Images C and D are examples of fibrous zeolite bundles images representing 30 % of the FZP observed, the majority featuring a splayed appearance with fibrils radiating from interconnected ends. Representative images of fibril-like structures are depicted in Images E and F. These are the most frequently detected amongst the FZPs (56 %), many of which are dispersed around FZP aggregates and bundles. The FZPs observed in this study bear a strong resemblance to the SEM images and descriptions of erionite found in the scientific literature, displaying fine, thin, rigid and elongated fibrous shapes [14,34,56]. It was observed that the axis of the elongated bundles or fibril-like structures are deposited along the plane of the leaf surfaces in Fig. 2, Image F.

3.2. Fibrous zeolite particles size distribution

The size distributions of the FZPs found on the leaf surfaces in the study area are presented in Table 3. The majority (92.2 %) of the FZPs were shorter than 5 μm in length; the width of the majority (91.5 %) of the FZPs was smaller than 1 μm. In this study, the particles that contained fine fibrils were also included in the FZPs (e.g. aggregates), thus, 78 % of FZP showed elongated shape with the aspect ratio being > 3 (Table 4).

3.3. Comparison with airborne zeolite fiber sizes reported in the literature

The FZPs observed in this study appear to be shorter than the airborne zeolite fibers reported in the literature (Table 5) [7,19,23]. Baris et al. [7] conducted a study at the epidemic center of malignant mesothelioma in three Turkish villages (Karain, Karlik and Sarihidir), reported the length of ~50 % of airborne zeolite fibers were greater than 5 μm; in our study, this proportion was 7.8 %. The average length of FZPs in this study (2.04 μm) was also shorter than that of the erionite air samples collected from both North Dakota (2.2 μm) and the three Turkish villages (3.57 μm) (Table 5) [19].

The width of majority (80.5 %) of the FZPs observed in this study were smaller than 0.5 μm, while the same size range was reported at around 40 % of the zeolite fibers found in the three Turkish villages (Karain 37.4 %, Karlik 44.3 % and Sarihidir 39.3 %, respectively). However, the average width (0.59 μm) of FZPs observed in this study was greater than those of the erionite fibers (0.31 μm) sampled from North Dakota and the Turkish villages [19] (Table 5). The discrepancy in the average width of the fibrous particles may be due to the inclusion of the fibrous zeolite particles in the shape of aggregates (Fig. 2 A and B), which generally has a greater width and smaller aspect ratios. In general, the majority of FZPs observed in this study were smaller compared to those airborne erionite fibers reported in previous studies.

It is worth noting that in this study, the sizes of the FZPs were measured using SEM topographic viewed images, which may differ from the fiber sizes measured from North Dakota and the Turkish villages, which were measured using TEM [19]. Further experiments, using standard instruments for measuring airborne samples are needed to compare the differences between the measurements quantitatively. SEM based analytical protocols are commonly used to detected and quantify asbestos fibers in bulk samples, airborne samples and other matrices [60,74–76].

3.4. Similarities in energy-dispersive X-ray spectrometry (EDX) spectra

The EDX spectra of the FZPs from the leaf surfaces and the bulk

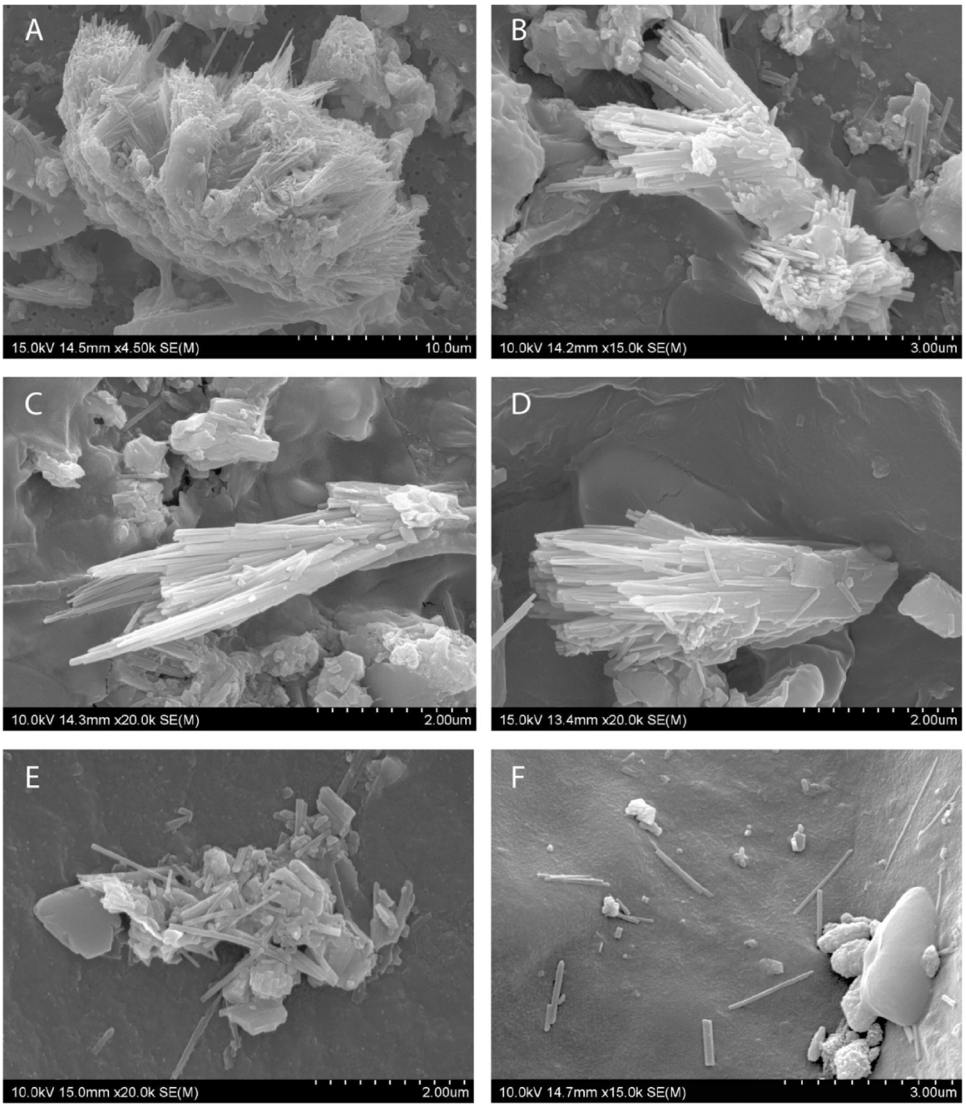

Fig. 2. : Example SEM micrographs of fibrous zeolite particles detected on leaf surfaces. **A,B**. Fibrous aggregates. **C,D**. Fiber bundles. **E,F**. Fibril-like structures.

Table 3
Fibrous zeolite particle size distribution (%). Size was measured using SEM micrographs.

Length / Width (μm)	< 0.1	0.1– 0.5	0.5 – 1	1 – 3	> 3
1 – 5	44.3	35.6	8.4	3.9	—
5 – 10	0.3	1.3	1.3	2.3	0.6
10 – 20	—	—	0.3	0.6	0.3
> 20	—	—	—	—	0.6

Table 4
Aspect ratio (length/width) distribution of the fibrous zeolite particles detected.

Aspect Ratio	< 3	3–10	10–20	20–30	30–40	> 40
Percentage %	22	46	22	7	2	1

samples that contain erionite/mordenite were similar, as shown in Fig. 3. We noted major peaks for oxygen (O), silicon (Si) and aluminum (Al), minor peaks for potassium (K), sodium (Na), calcium (Ca) and magnesium (Mg). This is consistent with a statement presented in a previous study that it is difficult to differentiate fibrous zeolites based only on their EDX spectra [35]. Therefore, for the FZPs that meet both the morphological and elemental identification criteria, further differentiation requires detailed calculations of their elemental composition.

3.5. Mineralogical methodologies for differentiating fibrous zeolites

Identifying different zeolites, e.g., differentiating erionite from mordenite and offretite, often involves detailed investigations into the elemental compositions of these zeolites. Passaglia [77] proposed using (Si+Al) ≈ 36 with a balance error (E%) (Eq. 2) of less than 10 % to reliably identify erionite using chemical composition analysis [78,79, 77,80].

$$E\% = \frac{\left(Al + Fe^{3+}\right) - Na + K + 2 \times (Ca + Mg + Sr + Ba)}{Na + K + 2 \times (Ca + Mg + Sr + Ba)} \times 100 \quad (2)$$

However, these criteria may have limited application for identifying individual airborne zeolite fibers, particularly for air samples with small sample volumes and fiber sizes. For instance, in the erionite air samples collected from Cappadocia, Turkey, 82 % did not meet the E% ≤ 10 % [32].

3.6. Differentiate fibrous zeolites using the tetrahedral Si/(Si + Al) ratio

The tetrahedral Si/(Si+Al) ratio (Tsi or R ratio) is an important

Table 5
Comparison of size distribution between fibrous particles found in this study and those reported in the literature.

Location	Sample	Length (μm)			Width (μm)			Aspect ratio		
		Min	Mean	Max	Min	Mean	Max	Min	Mean	Max
New Zealand	Zeolite	0.26	2.04	24.3	0.02	0.59	20.9	0.85	9.08	43.75
North Dakota, USA [19]	Erionite	0.56	2.20	16.8	0.05	0.31	1.28	3.00	7.61	28.33
Turkey [19]	Erionite	0.56	3.57	38.1	0.06	0.31	5.04	2.5	20.46	370

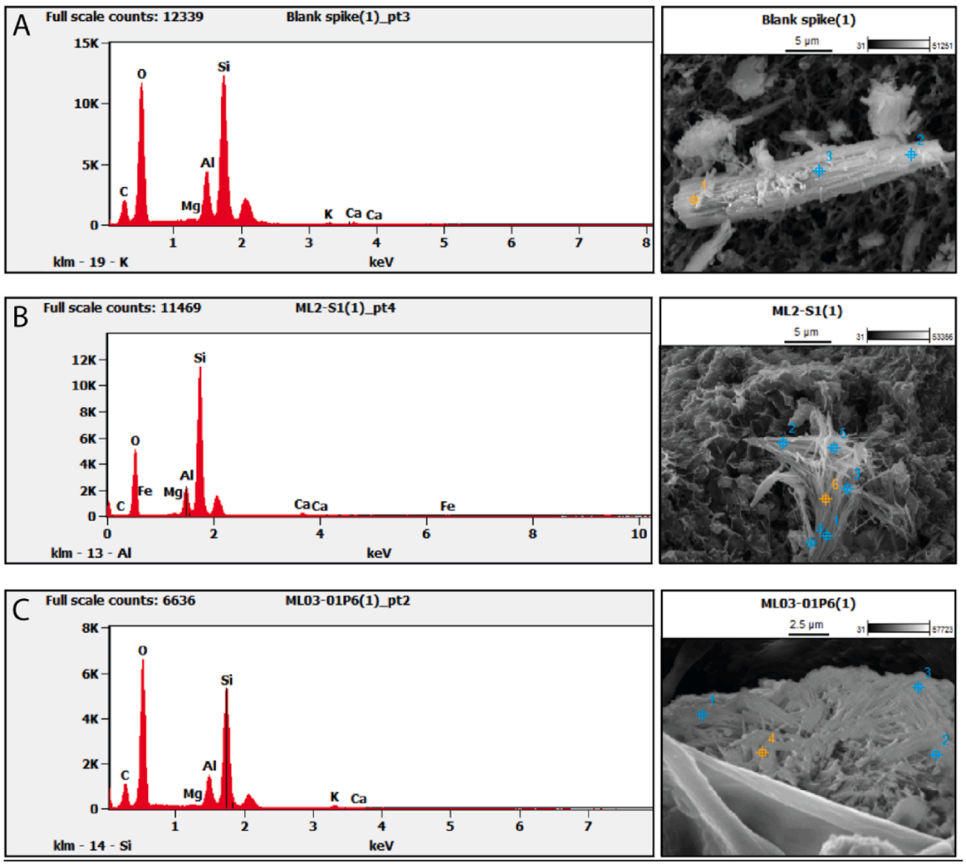

Fig. 3. Examples of the SEM-EDX elemental spectrum of three types of samples tested. **A**. Erionite containing bulk sample. **B**. Mordenite containing bulk sample. **C**. Fibrous zeolite particles on leaf surface. Each panel shows the EDX spectra and the corresponding SEM images of the particles that were tested.

parameter for distinguishing different fibrous zeolites [4,49,50]. This ratio was calculated for both FZPs and the mordenite and erionite containing bulk samples using the Si and Al element weight percentage (wt %) obtained from SEM-EDX results. Pacella et al. [49] demonstrated the relative stability of Si and Al measurements in SEM-EDX analysis, even for particles with diameters smaller than 8 μm. It was observed that Si weight percentages of those small particles were consistent with the results of the bulk samples across various zeolite types (natrolite, scolecite, leucite and nepheline) [49]. However, a decrease of approximately 6 % was noted in the Al weight percentage in smaller particles (diameter < 1 μm) and a reduction of around 1 % in the Al weight percentage in larger zeolite particles (diameter 1– 8 μm) compared to the results from the bulk sample tested [49].

The Tsi values of the particles derived from the control erionite containing bulk samples (Fig. 4) fell within the reference range for erionite (0.68 – 0.74); while the Tsi values obtained from the control mordenite bulk samples aligned roughly with the reference range for mordenite (0.80 – 0.86) [50]. However, for the FZPs (Samples 1– 24) collected from the leaf surfaces, 40 % of the Tsi ratios fell within the mordenite reference range, with only one sample within the erionite reference range [50]. Surprisingly, 80 % of the FZPs that displayed Tsi values associated with ferrierite (0.80 – 0.88), another fibrous zeolite type that has not been reported geological occurrence in the study area [10,50]. Further investigation revealed that the FZP with the low Tsi ratio (0.74) was found next to a larger rock particle with a higher Al content. This suggests that the low Tsi ratio of the particle may be due to potential background aluminum signal detection [81].

As indicated in Fig. 4, both erionite and mordenite containing bulk samples exhibited a tendency toward the upper range of their Tsi values as suggested in literature [50]. Several factors may contribute to the potential higher Tsi ratios calculated using EDX results. Firstly, the reduction in Al weight percentage in 'smaller particles' (diameter < 1 μm), as noted in Pacella et al. [49], may contribute to higher Tsi ratios. In this study, 91.5% of the ZFPs exhibited widths equal to or less than 1 μm, which could potentially lead to a higher Tsi ratio. Secondly, previous studies suggest that sedimentary zeolites often exhibit higher Tsi values, compared to zeolites derived from vesicles in volcanic rocks [4, 19,34,40,82,83]. For example, in Carbone et al. [19], the Tsi values of the majority of sedimentary erionite samples collected from North Dakota and the Old Sarihidir village in Turkey were within the range of 0.76 – 0.82, which is higher compare to the erionite reference value (0.68 – 0.74) suggested Coombs et al. [50] The zeolites in Ngakuru area were reported as sedimentary deposits, which could also potentially result in higher Tsi ratios compared to the zeolite reference values

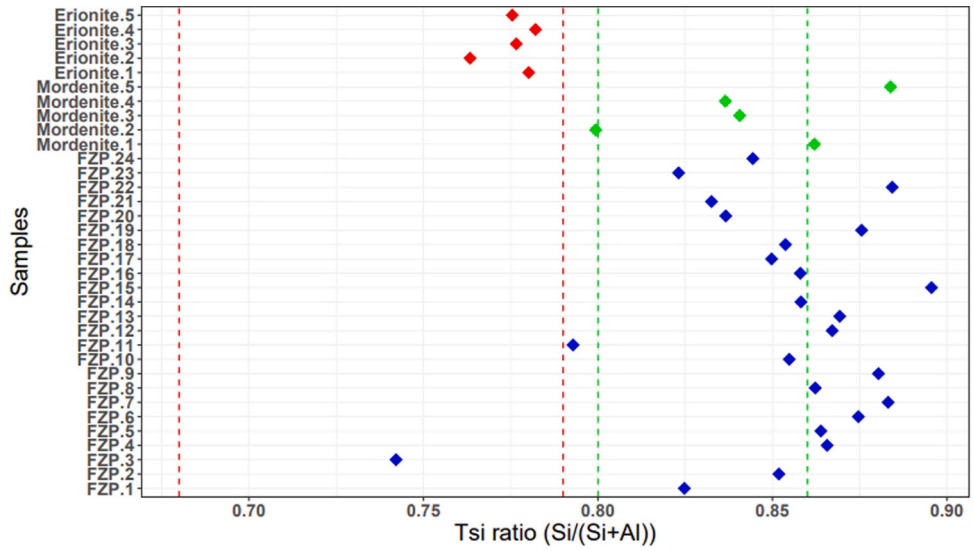

Fig. 4. Tsi ratio results of 24 FZPs (blue points) detected from leaf surfaces and 5 of erionite (red points) and mordenite bulk samples (green points). The red dashed lines indicate erionite Tsi ratio range (0.68–0.79), and the green dashed lines indicate mordenite Tsi ratio range (0.8–0.86), as suggested in Coombs et al. (1998).

suggested in the literature [55]. This introduces uncertainties for accurate FZP identification.

3.7. Differentiation of fibrous zeolites by TEM-SAED

Due to the variations in Tsi ratios in the SEM-EDX analysis results, which may be potentially caused by the size and geological formations of the zeolites, further examination is necessary to identify FZPs found on leaf surfaces. Mineralogists recommended the SAED technique as a more reliable method for distinguishing between fibrous zeolites based on differences in their crystal unit cell parameters [9,35,78]. Thus, TEM-SAED analysis using MicroED was performed in this study to identify individual zeolite fibers based on their crystallographic unit cell.

3.7.1. Results from the direct transfer method

Using the direct transfer method, a total of 34 electron diffraction (ED) datasets were collected on elongated shaped fibers, including those for the control erionite (n = 14) and mordenite (n = 7) containing bulk samples, as well as the FZPs (n = 13) from the leaf surfaces (Table 6). Among the 34 sets of datasets, 11 (32%) were successfully identified, indexed with the unit-cell parameters corresponding to erionite, mordenite, offretite, or nontronite. Nine of the data sets (26%) indexed with unit-cell parameters of minerals did not match those of natural zeolites or common layer silicates, while 14 of the datasets (41%) failed to index.

Of the14 ED datasets collected from the erionite bulk samples, three were assigned to the unit-cell parameters that matched the reference values for erionite in literature, two were assigned to offretite, and one was assigned to the mineral nontronite, which belongs to the smectite group and is a common clay-like mineral found alongside zeolites (https://www.mindat.org/min-2924.html) [33]. The co-existence of offretite with erionite is consistent with the literature [9]. However, in this study, offretite was not in the XRPD report of the erionite bulk sample (see S1 in the Supporting Information). This may be due to a very low concentration of offretite (below the detection limit of XRPD), or due to the similarities between the XRPD patterns of offretite and erionite, leading to the non-detection of offretite [62].

The mordenite containing bulk samples showed only one match with the reference mordenite unit-cell parameters [39,71]. Four crystals had the unit-cell parameters of a = 6.8 Å; b = 9.5 Å; c = 12.9 Å; α = 75°; β = 90°; γ = 90°, which is not a match to any known zeolites identified in the literature. Thus, the identity of these four crystals remains ambiguous.

Table 6
The crystal unit cell parameter results of 34 fibers analyzed using the direct transfer method.

Sample ID	*a* (Å)	*b* (Å)	*c* (Å)	*α* (°)	*β* (°)	*γ* (°)	Prediction
Erionite.1	13	13	15	90	90	120	Erionite
Erionite.2	13	13	7.5	90	90	120	offretite
Erionite.3	13	13	7.5	90	90	120	offretite
Erionite.4	-	-	-	-	-	-	No-index
Erionite.5	-	-	-	-	-	-	No-index
Erionite.6	13	13	15	90	90	120	Erionite
Erionite.7	13	13	15	90	90	120	Erionite
Erionite.8	5.2	5.2	10.2	90	95	120	Unknown
Erionite.9	-	-	-	-	-	-	No-index
Erionite.10	-	-	-	-	-	-	No-index
Erionite.11	-	-	-	-	-	-	No-index
Erionite.12	-	-	-	-	-	-	No-index
Erionite.13	6.5	6.8	9.4	90	75.7	89.9	Unknown
Erionite.14	5.2	9.1	10.2	89.4	100.8	89.6	Nontronite
Mordenite.1	18	20	7.5	90	90	90	Mordenite
Mordenite.2	16.5	6.8	9.9	90	104	90	Unknown
Mordenite.3	-	-	-	-	-	-	No-index
Mordenite.4	6.8	9.5	12.9	75	90	90	Unknown
Mordenite.5	6.8	9.5	12.9	75	90	90	Unknown
Mordenite.6	6.8	9.5	12.9	75	90	90	Unknown
Mordenite.7	6.8	9.5	12.9	75	90	90	Unknown
FZP.1	-	-	-	-	-	-	No-index
FZP.2	-	-	-	-	-	-	No-index
FZP.3	-	-	-	-	-	-	No-index
FZP.4	3.7	13	13	90	90	90	Unknown
FZP.5	-	-	-	-	-	-	No-index
FZP.6	18	20.4	7.5	90	90	90	Mordenite
FZP.7	-	-	-	-	-	-	No-index
FZP.8	11.3	14	14.2	92.4	105.8	105.8	Unknown
FZP.9	-	-	-	-	-	-	No-index
FZP.10	-	-	-	-	-	-	No-index
FZP.11	18.2	20.2	7.6	90	90	90	Mordenite
FZP.12	18.1	20.2	7.6	90	90	90	Mordenite
FZP.13	18.2	20.4	7.6	90	90	90	Mordenite

Of the 13 FZPs sampled from the leaf surfaces (Table 6), four showed unit-cell parameters consistent with mordenite [6,63]. No other zeolite minerals were identified in the FZPs from leaf surfaces.

Notably, 38 % of the ED datasets collected using the direct transfer method could not be indexed. This was mainly due to weak diffraction data or challenges associated with finding an isolated individual zeolite crystal. The failure to index can also be attributed to the overlapping of

crystals, or crystals being in less ideal positions on the grid, which can restrict the range of data collection due to TEM sample stage tilting limitations [33,84,85]. The main obstacle in analyzing FZPs from the leaf surfaces using the direct transfer method was the small particle sizes and the low particle density on the TEM grid. Single zeolite fibrils are extremely fine, small crystalline structures. To prevent electron beam damage, samples were examined under cryogenic conditions (−170 °C), using TEM low dose mode and a 200 μm select area aperture. This may have reduced the diffraction intensity, and the lack of strong reflections can impede successful data indexing and integration.

3.7.2. Results from the indirect transfer method

To improve diffraction data quality and enhance the accuracy of zeolite identification based solely on crystallographic data, the indirect transfer method was performed on 10 sets of erionite-containing bulk samples and 10 sets of FZPs from leaf surface samples collected at the TL01 sampling location (Fig. 1).

The results (Table 7) show that 8 out of 10 fibers tested using the indirect transfer method from the erionite-containing bulk samples were successfully indexed and identified as erionite. One fiber was identified as offretite, while another could not be indexed, likely due to the presence of multiple crystal lattices in different orientations, causing smearing of diffraction spots. All ten FZPs from the leaf surfaces were indexed as mordenite (Table 7). Examples of continuous rotation diffraction data in video format for erionite and mordenite are provided in S8 and S9 in the Supporting Information.

The TEM grid prepared using the indirect transfer method showed a higher number of transferred FZPs and reduced the fiber search time. These fibers were longer and had a greater aspect ratio compared to those obtained by the direct transfer method (Fig. 5). Additionally, there was a notable increase in the number and sharpness of diffraction spots due to the higher electron beam intensity and smaller aperture used, which reduced background scattering. However, the level of potential chemical contamination remains uncertain, given the high absorbance capacity of zeolites, and the impact of radiation damage on subsequent chemical analysis is yet to be determined.

Both direct and indirect transfer methods enable researchers without specialized expertise in crystallography to identify environmental fibrous zeolites. By using indexing software (XDS) to analyze continuous rotation diffraction data collected by MicroED, fibers can be identified based on their repeating crystallographic cell unit parameters (a, b, c, α, β, γ). The direct transfer method is straightforward in sample preparation, has minimal impact on chemical composition, and the cryogenic conditions allow for extended ED data collection and further EDS analysis. Meanwhile, the indirect method involves more complex sample preparation and increased electron beam intensity, which significantly enhances ED data quality and indexing success rates, thereby improving the accuracy of erionite identification.

Table 7
The crystal unit cell parameter results of 20 fibers analyzed using the indirect transfer method.

Sample ID	a (Å)	b (Å)	c (Å)	α (°)	β (°)	γ (°)	Prediction
Erionite.15	13	13.1	15.1	89.8	89.8	120	Erionite
Erionite.16	13.4	13.4	15.1	90	90	120	Erionite
Erionite.17	13.3	13.2	15.4	90	90	120	Erionite
Erionite.18	13.1	13.1	15.4	90	90	120	Erionite
Erionite.19	13.2	13.2	15.5	90	90	120	Erionite
Erionite.20	13.2	13.2	15.5	90	90	120	Erionite
Erionite.21	13.2	13.2	15.1	90	90	120	Erionite
Erionite.22	13.4	13.4	15.2	90	90	120	Erionite
Erionite.23	13.1	13.2	7.6	90	90	120	offretite
Erionite.24	-	-	-	-	-	-	No-index
FZP.14	17.6	20.4	7.6	90	90	90	Mordenite
FZP.15	18	20.7	7.5	90	90	90	Mordenite
FZP.16	17.8	20.7	7.5	90	90	90	Mordenite
FZP.17	18.1	20.7	7.5	90	90	90	Mordenite
FZP.18	18.2	20.2	7.5	90	90	90	Mordenite
FZP.19	18	20.3	7.6	90	90	90	Mordenite
FZP.20	18.2	20.3	7.6	90	90	90	Mordenite
FZP.21	17.9	20.3	7.6	90	90	90	Mordenite
FZP.22	18.2	20.4	7.5	90	90	90	Mordenite
FZP.23	17.9	20.4	7.6	90	90	90	Mordenite

3.8. Spatial variance across the sampling stations

FZPs were detected on the tree leaf surfaces of 12 of the 15 sampling sites in this study, with the average and maximum number of particles per square centimeter on the leaf surfaces being 4905 and 48,541 n/cm^2, respectively (Fig. 6). The highest abundance of FZPs on the leaf surface was observed at the TL01 (Fig. 1), with values of 28,333 ± 20,208 n/cm^2, while the lowest abundances (non-detected) were found at ML01, ML02 and NL03 (Fig. 6). The leaf samples collected from the locations around the active quarry close to the Twist Road and Rehi Road showed higher levels of FZP deposition (10,158 ± 1579 /cm^2) compared to the samples collected from locations around the non-active quarries on the Mangatete Road (1944 ± 389 /cm^2) (Fig. 1). Note that these numbers of FZPs per centimeter of leaf surface across the sampling stations are only for the time of sample collection (15th March 2023). Thus, they represent only an estimation of FZP abundance, and do not account for factors such as local differences in rainfall, wind speed and direction, as well as differences in vegetation characteristics such as leaf shape, size, orientation, and surface friction that will all likely affect the deposition rates and rate of particle retention on the leaf's surface.

The emission sources of the FZPs detected on the leaf surface remain unclear. Although, a greater abundance of FZPs were detected around the active zeolite quarry, no significant positive correlation was found between the distance to the quarries and the levels of the FZPs on the leaf surfaces. However, further work is required to quantitatively sample fibers found to establish these types of patterns in spatial and temporal abundance. Interestingly, similar observations were reported in an erionite exposure study conducted in Turkish villages. Stationary air samplers located away from the road (with no immediate disturbance) showed 'not detected' results in areas with erionite containing rocks present [7,19,26]. This suggests that factors such as the meteorological conditions and the distance from the roads may influence FZP levels, indicating the complexity of fibrous particle dispersion dynamics in ambient environments. Future studies should consider geological and meteorological factors, and collect repeated data at shorter intervals and different heights to more accurately reflect spatial variations in fibrous zeolite particle deposition on leaf surfaces.

In addition to fibrous zeolites, other mineral particles, including pumice and diatomaceous earth, were also detected on the leaf surfaces (S7 in Supporting Information). This finding aligns with the geological descriptions of mineral occurrence in the region, as documented in previous studies [55,56]. Pumice, in particular, emerged as the most abundant mineral on the leaf surface samples collected from the Mangatete Road (ML01 - 06) sampling stations. In contrast, fibrous zeolite particles dominated the leaf surface samples collected from the Twist and Rehi Road sampling locations.

3.9. Implications

Some naturally occurring mineral fibers such as asbestos, fluoroedenite, and erionite are classified as *Group 1* carcinogens, presenting significant risks to humans [87,88]. Despite their typical low ambient concentrations, disturbance-induced inhalation poses notable health hazards [19,87,88]. Erionite is found in over 150 locations worldwide, including in densely populated cities like Auckland, New Zealand, where the bed rocks and sediments containing erionite may be increasingly disturbed as the scale of urban development into greenfield sites increases [29,89,90].

Recent measurement and modeling suggests that wind erosion can transport erionite-containing particles over long distances [91–93].

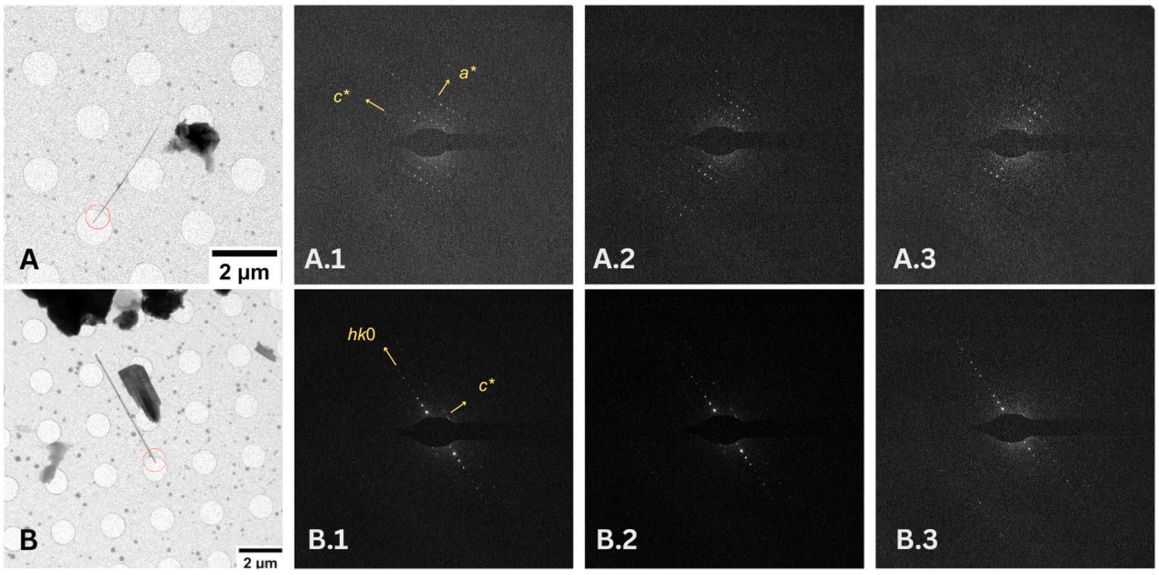

Fig. 5. TEM images of Zeolite fibers and their associated SAED patterns (indirect transfer method). **A**. Erionite fiber from erionite containing bulk sample and three concurrent SAED patterns (A.1,2,3) collected at 0.6° tilt increments. **B.** Mordenite fiber collected from leaf surface and its associated SAED patterns (B.1,2,3) at 0.6° tilt increments. A.1 is a diffraction pattern of erionite showing the a^* , c^* direcions [33]. B.1 is a diffraction pattern of mordenite showing the $hk0$ and c^* directions [86].

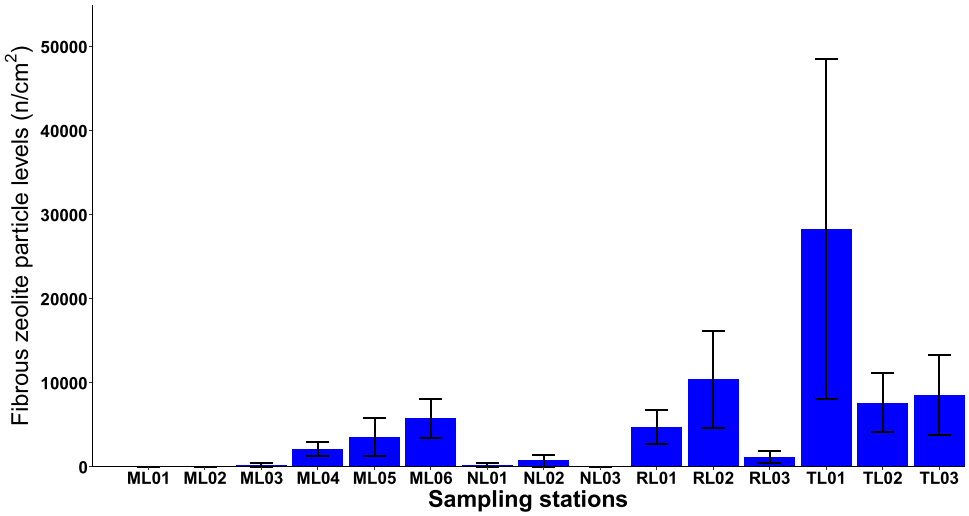

Fig. 6. The fibrous particles levels on leaf surfaces across the sampling locations. The columns represent the mean value and the error bars indicate the standard error.

Given these risks, monitoring airborne hazardous mineral levels in high-risk areas is crucial. Existing occupational health and safety equipment is not suitable for ambient air monitoring and is costly to operate and maintain, making it unsuitable for the frequent screening of large areas. This study presents a low-cost methodology for effectively detecting the presence of naturally occurring airborne hazardous minerals in ambient air.

The results show that these methods can be used to detect the presence of, and characterize, the atmospheric dispersion of naturally occurring fibrous mordenite deposited on leaf surfaces located alongside roadways in an area with volcaniclastic geology. Although the abundance of fibers varied across the 15 sampling stations and was likely influenced by multiple factors (including different tree species and distance to road), the presence of deposited fibers in this environment is significant. While these results are not quantitative and cannot be directly compared to regulatory standards or guidelines, the novel approach provides indicative data on the presence of respirable-sized crystalline fibrous zeolites in ambient air at the studied locations and highlights the need for further quantitative measurement and modelling investigations.

Moreover, this methodology is relatively easy to operate. Direct SEM scanning of leaf surfaces prevents potential contamination and sample loss during fiber extraction processes compared to other unconventional ambient air mineral fiber detection methods, such as animal lung deposition and tree bark deposition sampling [93,94]. Additionally, MicroED analysis enables the identification of individual zeolite fibers and the differentiation of erionite from other fibrous zeolites. The direct transfer method using cryo-conditions could be advantageous in scenarios where subsequent EDS analysis is required, while the indirect transfer method significantly increases the accuracy of indexing and identifying zeolite fibers.

4. Conclusions

Zeolite minerals, abundant in the natural dust, may pose a respiratory risk to humans, particularly when in fine fibrous form. This study, carried out in the Taupo Volcanic Zone of New Zealand, introduces a novel methodology combining leaf surface sampling and electron microscopic analysis to assess the presence of aerosolized zeolite fibers in the area.

In total, 309 fibrous zeolite particles (FZPs) were detected in 12 out of 15 sampling stations. The identified FZPs exhibited diverse morphologies, ranging from fibrous aggregates to fibril-like structures. The majority were less than 5 μm in length and notably smaller than those reported on in existing literature. SEM-EDX analysis showed that these FZPs shared elemental composition similarities with the confirmed erionite and mordenite containing bulk samples. Utilizing the relative stableness of Si and Al in EDX detection, the Tsi ratio indicated that over 40 % of the FZPs detected on leaf surfaces are likely to be mordenite.

Two methods of TEM-SAED analysis with Micro-ED enabled the identification of individual unknown mineral crystals or fibers from bulk and leaf samples as being erionite, mordenite, and offretite. Using the direct transfer method, 30 % of the tested FZPs were confirmed as mordenite, while 100 % of the tested FZPs were confirmed as mordenite using the indirect transfer method. Scholars suggest that incorporating TEM-EDS analysis with TEM-SAED Micro-ED analysis can further increase the accuracy of zeolite identification [33,35]. The direct transfer method minimizes potential chemical contamination and electron beam damage to fibers, allowing for subsequent TEM-EDS analysis.

In summary, the sampling of mineral dust that has settled on leaf surfaces and the direct scanning of these samples using SEM offers a cost-effective method for detecting the likely presence of airborne fibrous minerals in outdoor environments. It is acknowledged that this approach has limitations due to environmental uncertainties, preventing it from providing quantitative levels of hazardous mineral fibers for regulatory comparison. However, it remains applicable for screening regions with naturally occurring carcinogenic mineral fibers, such as erionite, where temporally and spatially heterogeneous samples of low concentrations are expected in ambient air. This cost-effective method is thus a useful first step for identifying areas for standard quantitative sampling of hazardous mineral fibers and providing insights into the needs for future human exposure investigations.

Environmental Implication

When disturbed, naturally occurring fibrous zeolites (such as erionite, a *Group 1* carcinogen) in rocks and soil may present a significant risk to human health. Understanding the spatial abundance and characteristics of these airborne fibers is crucial for assessing risk and minimizing human exposure. Traditional monitoring methods for similar airborne hazardous fibers, developed and used in industrial settings, are costly and unsuitable for large-scale screening in low-concentration outdoor environments. This study presents a novel, low-cost sampling approach for these settings, which draws on particulate deposits on leaf surfaces and is effectively used to detect and characterize hazardous fibers.

CRediT authorship contribution statement

Alessandro F. Gualtieri: Writing – review & editing, Methodology, Formal analysis. **Kim N. Dirks:** Writing – review & editing, Supervision, Conceptualization. **Paul G. Young:** Methodology, Formal analysis. **Jennifer A. Salmond:** Writing – review & editing, Supervision, Funding acquisition, Conceptualization. **Wenxia (Wendy) Fan:** Writing – review & editing, Writing – original draft, Visualization, Methodology, Investigation, Formal analysis, Data curation, Conceptualization.

Declaration of Competing Interest

The authors declare the following financial interests/personal relationships which may be considered as potential competing interests: Wenxia (Wendy) Fan reports financial support was provided by Ministry of Business Innovation and Employment. If there are other authors, they declare that they have no known competing financial interests or personal relationships that could have appeared to influence the work reported in this paper.

Data Availability

Data will be made available on request.

Acknowledgements

This work was funded by a New Zealand Ministry of Business Innovation and Employment Endeavour Grant, number UOAX2009, entitled ‘Assessing and Managing the Risk of Carcinogenic Erionite in New Zealand’. The authors express gratitude to Janki Patel for providing erionite-containing bulk samples, Dr. Yuan Tao for technical assistance during the SEM-EDX analysis, and Dr. Adrian Turner for instrument support during the TEM analysis. Finally, authors warmly thank the editor and the three reviewers for their suggestions and support during the revision of the manuscript.

Appendix A. Supporting Information

Supporting Information associated with this article can be found in the online version at doi:10.1016/j.jhazmat.2024.135982.

References

[1] Bish, D.L., Ming, D.W. (Eds.), 2001. Natural Zeolites: Occurrence, Properties, Applications. Reviews in Mineralogy and Geochemistry vol. 45. Washington, DC: Mineralogical Society of America. Geochemical Society.
[2] Inglezakis, V.J., Zorpas, A.A. (Eds.), 2012. Handbook of Natural Zeolites. Bentham Science Publishers.
[3] Marantos, I., Christidis, G.E., Ulmanu, M., 2012. Zeolite formation and deposits. : Handb Nat Zeolites 28–51.
[4] Bish, D.L., Guthrie Jr., G.D., 1993. Minerology of clay and zeolite dusts (exclusive of 1:1 layer silicates). *Health Effects of Mineral Dusts*. De Gruyter, Berlin, Boston, pp. 139–184. https://doi.org/10.1515/9781501509711-007.
[5] Guthrie Jr., G.D., 1992. Biological effects of inhaled minerals. Am Mineral 77, 225–243.
[6] Giordani, M., Ballirano, P., Pacella, A., Meli, M.A., Roselli, C., Di Lorenzo, F., Fagiolino, I., Mattioli, M., 2022. Another potentially hazardous zeolite from northern Italy: fibrous mordenite. Minerals 12 (5), 627. https://doi.org/10.3390/min12050627.
[7] Baris, I., Artvinli, M., Saracci, R., Simonato, L., Pooley, F., Skidmore, J., Wagner, C., 1987. Epidemiological and environmental evidence of the health effects of exposure to erionite fibres: a four-year study in the Cappadocian region of Turkey. Int J Cancer 39 (1), 10–17. https://doi.org/10.1002/ijc.2910390104.
[8] Dogan, A.U., Dogan, M., Hoskins, J.A., 2008. Erionite series minerals: mineralogical and carcinogenic properties. Environ Geochem Health 30 (4), 367–381. https://doi.org/10.1007/s10653-008-9165-x.
[9] Gualtieri, A., Artioli, G., Passaglia, E., Bigi, S., Viani, A., Hanson, J.C., 1998. Crystal structure-crystal chemistry relationships in the zeolites erionite and offretite. Am Mineral 83 (5–6), 590–606. https://doi.org/10.2138/am-1998-5-618.
[10] Gualtieri, A.F., Gandolfi, N.B., Passaglia, E., Pollastri, S., Mattioli, M., Giordani, M., Ottaviani, M.F., Cangiotti, M., Bloise, A., Barca, D., Vigliaturo, R., 2018. Is fibrous ferrierite a potential health hazard? Characterization and comparison with fibrous erionite. Am Mineral 103 (7), 1044–1055. https://doi.org/10.2138/am-2018-6508.
[11] Maher, B., 2010. Epidemiology: Fear in the Dust. Nature 468 (7326), 884–885. https://doi.org/10.1038/468884a.
[12] World Health Organization, 2017. WHO Guidelines on Protecting Workers from Potential Risks of Manufactured Nanomaterials. World Health Organization,.
[13] Baris, Y.I., Grandjean, P., 2006. Prospective study of mesothelioma mortality in Turkish villages with exposure to fibrous zeolite. JNCI: J Natl Cancer Inst 98 (6), 414–417. https://doi.org/10.1093/jnci/djj106.
[14] Carbone, M., Emri, S., Dogan, A.U., Steele, I., Tuncer, M., Pass, H.I., Baris, Y.I., 2007. A mesothelioma epidemic in Cappadocia: scientific developments and unexpected social outcomes. Nat Rev Cancer 7 (2), 147–154. https://doi.org/10.1038/nrc2068.

[15] IARC Working Group. The Evaluation of Carcinogenic Risks to Humans: Silica, Some Silicates, Coal Dust and Para-Aramid Fibrils. Lyon, 15–22 October 1996. IARC Monogr Eval Carcinog Risks Hum. 1997;68:1.
[16] Coffin, D.L., Cook, P.M., Creason, J.P., 1992. Relative mesothelioma induction in rats by mineral fibers: comparison with residual pulmonary mineral fiber number and epidemiology. Inhal Toxicol 4 (3), 273–300. https://doi.org/10.3109/08958379209145671.
[17] Wagner, J.C., Skidmore, J.W., Hill, R.J., Griffiths, D.M., 1985. Erionite exposure and mesotheliomas in rats. Br J Cancer 51 (5), 727–730. https://doi.org/10.1038/bjc.1985.108.
[18] Di Giuseppe, D., 2020. Characterization of fibrous mordenite: a first step for the evaluation of its potential toxicity. Crystals 10 (9), 769. https://doi.org/10.3390/cryst10090769.
[19] Carbone, M., Baris, Y.I., Bertino, P., Brass, B., Comertpay, S., Dogan, A.U., Gaudino, G., Jube, S., Kanodia, S., Partridge, C.R., Pass, H.I., 2011. Erionite exposure in North Dakota and Turkish villages with mesothelioma. Proc Natl Acad Sci 108 (33), 13618–13623. https://doi.org/10.1073/pnas.1105887108.
[20] National Institute for Occupational Safety and Health (NIOSH) manual of analytical methods (NMAM), 5th edition [Internet]. [cited 2023 Apr 18]. Available from: ⟨https://stacks.cdc.gov/view/cdc/50253⟩.
[21] International Organization for Standardization. ISO 10312:2019 (en) Ambient air — Determination of asbestos fibres — Direct transfer transmission electron microscopy. ISO; 2019.
[22] International Organization for Standardization. ISO 13794:2019 (en) Ambient air — Determination of asbestos fibres — Indirect-transfer transmission electron microscopy. ISO; 2019.
[23] Rohl, A.N., Langer, A.M., Moncure, G., Selikoff, I.J., Fischbein, A., 1982. Endemic pleural disease associated with exposure to mixed fibrous dust in Turkey. Science 216 (4545), 518–520. https://doi.org/10.1126/science.7071597.
[24] Berman, D.W., Crump, K.S., Chatfield, E.J., Davis, J.M.G., Jones, A.D., 1995. The sizes, shapes, and mineralogy of asbestos structures that induce lung tumors or mesothelioma in AF/HAN rats following inhalation1. Risk Anal 15 (2), 181–195. https://doi.org/10.1111/j.1539-6924.1995.tb00312.x.
[25] Berman, D.W., Crump, K.S., 2008. A meta-analysis of asbestos-related cancer risk that addresses fiber size and mineral type. Crit Rev Toxicol 38 (sup1), 49–73. https://doi.org/10.1080/10408440802273156.
[26] Beaucham, C., King, B., Feldmann, K., Harper, M., Dozier, A., 2018. Assessing occupational erionite and respirable crystalline silica exposure among outdoor workers in Wyoming, South Dakota, and Montana. J Occup Environ Hyg 15 (6), 455–465. https://doi.org/10.1080/15459624.2018.1447116.
[27] Matassa, R., Familiari, G., Relucenti, M., Battaglione, E., Downing, C., Pacella, A., Cametti, G., Ballirano, P., 2015. A deep look into erionite fibres: an electron microscopy investigation of their self-assembly. Sci Rep 5 (1), 16757. https://doi.org/10.1038/srep16757.
[28] Mumpton, F.A., Ormsby, W.C., 1976. Morphology of Zeolite in Sedimentary Rocks by Scanning Electron Microscopy. Natural Zeolites. Pergamon Press, p. 119.
[29] Patel, J.P., Brook, M.S., Kah, M., Hamilton, A., 2022. Global geological occurrence and character of the carcinogenic zeolite mineral, erionite: a review. Front Chem 10, 1066565. https://doi.org/10.3389/fchem.2022.1066565.
[30] Sameshima, T., 1976. Zeolites in Tuff Beds of the Miocene Waitemata group. Natural Zeolites. Pergamon press,, Auckland province, New Zealand.
[31] Van Gosen, B.S., Blitz, T.A., Plumlee, G.S., Meeker, G.P., Pierson, M.P., 2013. Geologic occurrences of erionite in the United States: an emerging national public health concern for respiratory disease. Environ Geochem Health 35 (4), 419–430. https://doi.org/10.1007/s10653-012-9504-9.
[32] Dogan, M., 2012. Quantitative characterization of the mesothelioma-inducing erionite series minerals by transmission electron microscopy and energy dispersive spectroscopy. Scanning 34 (1), 37–42.
[33] Gualtieri, A., Artioli, G., Passaglia, E., Bigi, S., Viani, A., Hanson, J.C., 1998. Crystal structure-crystal chemistry relationships in the zeolites erionite and offretite. Am Mineral.
[34] Harper, M., Dozier, A., Chouinard, J., Ray, R., 2017. Analysis of erionites from volcaniclastic sedimentary rocks and possible implications for toxicological research. Am Mineral 102 (8), 1718–1726.
[35] Ray, R., 2020. Discerning erionite from other zeolite minerals during analysis. Environ Eng Geosci 26 (1), 133–139.
[36] Greer, H.F., Zhou, W., 2011. Electron diffraction and HRTEM imaging of beam-sensitive materials. Crystallogr Rev 17 (3), 163–185.
[37] Wang, S.X., Wang, L.M., Ewing, R.C., 2000. Electron and ion irradiation of zeolites. J Nucl Mater 278 (2), 233–241.
[38] Cichocka, M.O., Ångström, J., Wang, B., Zou, X., Smeets, S., 2018. High-throughput continuous rotation electron diffraction data acquisition via software automation. J Appl Crystallogr 51 (Pt 6), 1652–1661.
[39] Giordani, M., Mattioli, M., Ballirano, P., Pacella, A., Cenni, M., Boscardin, M., Valentini, L., 2017. Geological occurrence, mineralogical characterization, and risk assessment of potentially carcinogenic erionite in Italy. J Toxicol Environ Health, Part B 20 (2), 81–103.
[40] Gottardi, G., Galli, E., Gottardi, G., Galli, E., 1985. Zeolites with 6-rings. Nat Zeolites 168–222.
[41] Dzierżanowski, K., Popek, R., Gawrońska, H., Sæbø, A., Gawroński, S.W., 2011. Deposition of particulate matter of different size fractions on leaf surfaces and in waxes of urban forest species. Int J Phytoremediat 13 (10), 1037–1046.
[42] Hofman, J., Bartholomeus, H., Janssen, S., Calders, K., Wuyts, K., Van Wittenberghe, S., Samson, R., 2016. Influence of tree crown characteristics on the local PM10 distribution inside an urban street canyon in Antwerp (Belgium): a model and experimental approach. Urban Urban Green 20, 265–276.
[43] Sæbø, A., Popek, R., Nawrot, B., Hanslin, H.M., Gawronska, H., Gawronski, S.W., 2012. Plant species differences in particulate matter accumulation on leaf surfaces. Sci Total Environ 427–428. :347–54.
[44] Lindén, J., Gustafsson, M., Uddling, J., Watne, Å., Pleijel, H., 2023. Air pollution removal through deposition on urban vegetation: the importance of vegetation characteristics. Urban Urban Green 81, 127843.
[45] Nurmamat, K., Halik, Ü., Baidourela, A., Aishan, T., 2022. Atmospheric particle distribution on tree leaves in different urban areas of Aksu City, Northwest China. Nat Environ Pollut Technol 21, 921–929.
[46] Salmond, J.A., Williams, D.E., Laing, G., Kingham, S., Dirks, K., Longley, I., et al., 2013. The influence of vegetation on the horizontal and vertical distribution of pollutants in a street canyon. Sci Total Environ 443, 287–298.
[47] Baron P.A. Measurement of Fibers. NIOSH manual of analytical methods. 5th edition; 2016 April; URL: ⟨https://stacks.cdc.gov/view/cdc/151249⟩.
[48] Hinds, W.C., 2012. Aerosol Technology: Properties, Behavior, and Measurement of Airborne Particles. John Wiley & Sons,.
[49] Pacella, A., Ballirano, P., Cametti, G., 2016. Quantitative chemical analysis of erionite fibres using a micro-analytical SEM-EDX method. Eur J Mineral 28 (2), 257–264.
[50] Coombs, D.S., Alberti, A., Armbruster, T., Artioli, G., Colella, C., Galli, E., Grice, J. D., Liebau, F., Mandarino, J.A., Minato, H., Nickel Passaglia E., Peacor D.R., Quartieri S., Rinaldi R., Ross M., Sheppard R.A., Tillmanns E., Vezzalini G., E.H., 1998. Recommended nomenclature for zeolite minerals: report of the subcommittee on zeolites of the international mineralogical association, commission on new minerals and mineral names. Mineral Mag 62 (4), 533–571.
[51] Jones, C.G., Martynowycz, M.W., Hattne, J., Fulton, T.J., Stoltz, B.M., Rodriguez, J. A., et al., 2018. The CryoEM method MicroED as a powerful tool for small molecule structure determination. ACS Cent Sci 4 (11), 1587–1592.
[52] Kabsch, W., 1993. Automatic processing of rotation diffraction data from crystals of initially unknown symmetry and cell constants. J Appl Crystallogr 26 (6), 795–800.
[53] Young, P.G., Smith, C.A., Sun, X., Baker, E.N., Metcalf, P., 2006. Purification, crystallization and preliminary X-ray analysis of Mycobacterium tuberculosis folylpolyglutamate synthase (MtbFPGS). Acta Cryst F 62 (6), 579–582.
[54] Brathwaite R. Zeolites in New Zealand and their uses as environmental minerals. Lower Hutt (NZ): GNS Science Report: 2017/27. 2017 Aug; 23. doi:10.21420/G2KP89.
[55] Brathwaite, R.L., 2003. Geological and mineralogical characterization of zeolites in lacustrine tuffs, Ngakuru, Taupo Volcanic Zone, New Zealand. Clays Clay Miner 51 (6), 589–598.
[56] Rodgers, K.A., Browne, P.R.L., Buddle, T.F., Cook, K.L., Greatrex, R.A., Hampton, W.A., et al., 2004. Silica phases in sinters and residues from geothermal fields of New Zealand. Earth-Sci Rev 66 (1), 1–61.
[57] Land Information New Zealand. NZ Contours (Topo, 1:50 k). Retrieved on 1st August 2024 from ⟨https://data.linz.govt.nz/layer/50768-nz-contours-topo-150k/⟩.
[58] NIWA (National Institute of Water and Atmospheric Research). CliFlo: NIWA's National Climate Database on the Web. Retrieved on 20th June 2023 from https://cliflo.niwa.co.nz/.
[59] Carter, L., 1971. Stratigraphy and sedimentology of the Waitemata Group, Puketotara Peninsula, Northland. NZ J Geol Geophys 14 (1), 169–191.
[60] Cossio, R., Albonico, C., Zanella, A., Fraterrigo-Garofalo, S., Avataneo, C., Compagnoni, R., et al., 2018. Innovative unattended SEM-EDS analysis for asbestos fiber quantification. Talanta 190, 158–166.
[61] Laskin, A., Cowin, J.P., 2001. Automated single-particle SEM/EDX analysis of submicrometer particles down to 0.1 μm. Anal Chem 73 (5), 1023–1029.
[62] Gualtieri, A., Artioli, G., Passaglia, E., Bigi, S., Viani, A., Hanson, J.C., 1998. Crystal structure-crystal chemistry relationships in the zeolites erionite and offretite. Am Mineral 83 (5–6), 590–606.
[63] Passaglia, E., 1975. The crystal chemistry of mordenites. Contr Miner Pet 50 (1), 65–77.
[64] Schneider, C.A., Rasband, W.S., Eliceiri, K.W., 2012. NIH Image to ImageJ: 25 years of image analysis. Nat Methods 9 (7), 671–675.
[65] Bagheri, G.H., Bonadonna, C., Manzella, I., Vonlanthen, P., 2015. On the characterization of size and shape of irregular particles. Powder Technol 270, 141–153.
[66] Rice, E.L., 1967. A statistical method for determining quadrat size and adequacy of sampling. Ecology 48 (6), 1047–1049.
[67] Wiegert, R.G., 1962. The selection of an optimum quadrat size for sampling the standing crop of grasses and forbs. Ecology 43 (1), 125–129.
[68] Armbruster, T., Gunter, M.E., 2001. Crystal structures of natural zeolites. Rev Mineral Geochem 45 (1), 1–67.
[69] Breysse, P.N., 1991. Electron microscopic analysis of airborne asbestos fibers. Crit Rev Anal Chem 22 (3–4), 201–227.
[70] Nannenga, B.L., 2020. MicroED methodology and development. Struct Dyn 7 (1), 014304.
[71] Fan, W., Salmond, J.A., Dirks, K.N., Cabedo Sanz, P., Miskelly, G.M., Rindelaub, J. D., 2022. Evidence and mass quantification of atmospheric microplastics in a coastal New Zealand City. Environ Sci Technol 56 (24), 17556–17568.
[72] Prata, J.C., da Costa, J.P., Duarte, A.C., Rocha-Santos, T., 2019. Methods for sampling and detection of microplastics in water and sediment: a critical review. TrAC Trends Anal Chem 110, 150–159.
[73] Kabsch, W., 2010. Integration, scaling, space-group assignment and post-refinement. Acta Crystallogr D Biol Crystallogr 66 (2), 133–144.

[74] Breysse, P.N., Cherrie, J.W., Addison, J., Dodgson, J., 1989. Evaluation of airborne asbestos concentrations using TEM and SEM during residential water tank removal. Ann Occup Hyg 33 (2), 243–256.
[75] Churg, A., 1982. Fiber counting and analysis in the diagnosis of asbestos-related disease. Hum Pathol 13 (4), 381–392.
[76] Gualtieri, A.F., Malferrari, D., Di Giuseppe, D., Scognamiglio, V., Sala, O., Gualtieri, M.L., Bersani, D., Fornasini, L., Mugnaioli, E., 2023. There is plenty of asbestos at the bottom. The case of magnesite raw material contaminated with asbestos fibres. Sci Total Environ 898, 166275.
[77] Passaglia, E., 1970. The crystal chemistry of chabazites. Am Mineral 55 (7–8), 1278–1301.
[78] Ballirano P., Bloise A., Gualtieri A.F., Lezzerini M., Pacella A., Perchiazzi N., Dogan M., Dogan A.U. The crystal structure of mineral fibres. In: Gualtieri A.F., editor. Mineral fibres: Crystal chemistry, chemical-physical properties, biological interaction and toxicity 2017 Jan. p. 17–64.
[79] Dogan, A.U., Dogan, M., 2008. Re-evaluation and re-classification of erionite series minerals. Environ Geochem Health 30 (4), 355–366.
[80] Passaglia, E., Artioli, G., Gualtieri, A., 1998. Crystal chemistry of the zeolites erionite and offretite. Am Mineral 83 (5–6), 577–589.
[81] Mu, S., Rafaelsen, J., 2019. Quantification and precision in particle analysis using SEM and EDS. Microsc Micro 25 (S2), 708–709.
[82] Gude, A.J., Sheppard, R.A., 1981. Woolly erionite from the Reese River Zeolite Deposit, Lander County, Nevada, and its relationship to other erionites. Clays Clay Miner 29 (5), 378–384.
[83] Sheppard, R.S., 1996. Occurrences of erionite in sedimentary rocks of the Western United States. US Geological Survey.
[84] Evans, P., 2006. Scaling and assessment of data quality. Acta Crystallogr D Biol Crystallogr 62 (1), 72–82.
[85] Leslie, A.G.W., Powell, H.R., Winter, G., Svensson, O., Spruce, D., McSweeney, S., et al., 2002. Automation of the collection and processing of X-ray diffraction data – a generic approach. Acta Crystallogr D Biol Crystallogr 58 (11), 1924–1928.
[86] Ormándi S., Cora I., Dallos Z., Kristály F., Dódony I. Structural study of mordenite from Mátra Mts. (N-Hungary): dachiardite moduls reduce channel size in mordenite. 2017 Nov 1 [cited 2024 Sep 21]; Available from: ⟨https://akjournals.com/view/journals/2051/2/1/article-p1.xm⟩.
[87] Belpoggi, F., Tibaldi, E., Lauriola, M., Bua, L., Falcioni, L., Chiozzotto, D., Manservisi, F., Manservigi, M., Soffritti, M., 2011. The efficacy of long-term bioassays in predicting human risks: Mesotheliomas induced by fluoro-edenitic fibres present in lava stone from the Etna volcano in Biancavilla, Italy | L'efficacia dei saggi a lungo termine nel predire i rischi per l'uomo. Mesot. Eur J Oncol 16 (4), 185–195.
[88] Carbone, M., Yang, H., 2012. Targeting mechanisms of asbestos and erionite carcinogenesis in mesothelioma. Clin Cancer Res 18 (3), 598–604.
[89] Patel, J.P., Brook, M.S., 2021. Erionite asbestiform fibres and health risk in Aotearoa/New Zealand: a research note. NZ Geogr 77 (2), 123–129.
[90] Brook M., Patel J., Black P., Salmond J., Dirks K., Berry T., et al. Zeolitic Erionite in New Zealand: Health Implications for Ground Engineering. In European Association of Geoscientists & Engineers; 2020 [cited 2021 Mar 4]. p. 1–5. Available from: ⟨https://www.earthdoc.org/content/papers/10.3997/2214–4609.202071060⟩.
[91] Aydar, E., Akkaş, E., 2022. The emission of natural harmful particulate matters by wind erosion and possible impact areas, Cappadocia province, Central Anatolia, Turkey. Bull Eng Geol Environ 81 (1), 20.
[92] Buck, B.J., Goossens, D., Metcalf, R.V., McLaurin, B., Ren, M., Freudenberger, F., 2013. Naturally occurring asbestos: potential for human exposure, Southern Nevada, USA. Soil Sci Soc Am J 77 (6), 2192–2204.
[93] Ward, T.J., Spear, T., Hart, J., Noonan, C., Holian, A., Getman, M., et al., 2006. Trees as reservoirs for amphibole fibers in Libby, Montana. Sci Total Environ 367, 460–465.
[94] Capella, S., Fornero, E., Bellis, D., Belluso, E., 2017. Analysis of respired amphibole fibers (asbestos and non-asbestos classified): discrimination between natural and anthropogenic sources using sentinel animals. Air Qual Atmos Health 10 (5), 533–542.